

Compton profiles for water and mixed water-neon clusters: A measure of coordinationM. Hakala,^{*,†} S. Huotari,[‡] K. Hämäläinen, and S. Manninen*Division of X-Ray Physics, Department of Physical Sciences, P.O.B. 64, FIN-00014 University of Helsinki, Finland*Ph. Wernet[§] and A. Nilsson*Stanford Synchrotron Radiation Laboratory, P.O. Box 20450, Stanford, California 94309, USA*

L. G. M. Pettersson

FYSIKUM, Albanova University Center, Stockholm University, S-10691 Stockholm, Sweden

(Received 24 February 2004; revised manuscript received 1 June 2004; published 17 September 2004)

Isotropic Compton profiles for a set of model structures comprising water molecules and isoelectronic neon atoms have been calculated using density-functional theory. We consider dimers at different intermolecular separations and clusters with a central water molecule surrounded by a coordination shell of 1-4 water molecules or neon atoms. For intermolecular distances typical of ice, the model structures lead to oscillations in the profile as compared with the profile of the corresponding free molecules/atoms. The isotropic Compton profile is shown to contain fundamental information on the local coordination in terms of the coordination number and distance of the molecules in the first coordination shell. In addition, we show that changes in the intramolecular O-H bond length of a free water molecule have an effect on the shape of the profile.

DOI: 10.1103/PhysRevB.70.125413

PACS number(s): 78.70.Ck, 71.15.Mb, 61.25.Em, 33.15.Dj

I. INTRODUCTION

Electron momentum densities in different materials can be measured by inelastic x-ray scattering at high energy and momentum transfers.^{1,2} From the scattering cross section one can extract the Compton profile $J(q)$, which, within the impulse approximation,³ is a two-dimensional integral of the momentum density $N(\mathbf{p})$ in a plane perpendicular to the scattering vector \mathbf{K} . The scattering vector is given by $\mathbf{K}=\mathbf{k}_1-\mathbf{k}_2$, where \mathbf{k}_1 and \mathbf{k}_2 are the wave vectors of the incoming and scattered photons, respectively. In covalently bonded and metallic systems the atomic and molecular wave functions become strongly perturbed upon the bond formation, leading to substantial effects in the Compton profile. In contrast, in weakly bonded systems, where cohesion takes place through hydrogen bonds or van der Waals interaction, the atomic and molecular wave functions to a large extent retain their original form. Although the resulting bond energies are small, the interactions lead to a specific steric arrangement of molecules, as exemplified by the local coordination of ice and the adsorption patterns of molecules on surfaces.⁴

The interesting question is how the weak bonding and the ensuing molecular arrangement are manifested in the Compton profile. The profile is expected to be affected by several phenomena: (i) the exchange interaction between the overlapping valence orbitals of the neighboring molecules, (ii) the polarization due to the electric field from the neighboring molecules, (iii) the charge transfer between the molecules, and (iv) the covalency. In the case of crystalline systems, Isaacs *et al.*⁵ have demonstrated that the anisotropy of the directional Compton profile of ice Ih exhibits oscillations related to the interaction between the molecules. The interpretation of the anisotropy by Isaacs *et al.*⁵ in terms of covalency has raised a discussion related to the nature of the hydrogen bond. It has been argued that the observed oscilla-

tions can most straightforwardly be interpreted as reflecting the antisymmetrization of the products of the monomer wave functions.⁶⁻⁸ Most interestingly, these studies have shown that nonhydrogen bonded systems, such as an argon crystal and “anti-ice”⁷ as well as a water-neon system,⁸ give rise to similar Compton profile anisotropies. In the anti-ice model the orientation of the water molecules was changed so that two hydrogen atoms as well as the lone pairs of two oxygen atoms face each other.⁷ These findings are in harmony with the principle of “bond oscillation”, suggested by Epstein and Tanner to explain the momentum densities and Compton profiles of molecules.⁹ According to this principle, chemical bonds induce oscillations in the momentum densities and Compton profiles along the bonding direction with a period inversely proportional to the bond length.

An important aspect of the hydrogen bond is the charge transfer. Barbiellini and Shukla¹⁰ have proposed a method to determine the amount of charge transfer from the Compton profile. They estimated the HOMO-LUMO mixing by studying the negative radial derivative of the isotropic momentum density for the free molecule, the dimer, a cluster and the ice crystal. They observed a systematic increase of charge transfer upon increasing the cluster size.

In the present work we focus on the oscillations induced by coordination and analyze in more detail how different kinds of steric arrangements (coordination number and nearest-neighbor distances) of molecules are reflected in the Compton profile. We use simplified model systems, which consist of water molecules and isoelectronic neon atoms, and concentrate on the spherically averaged Compton profiles, which are relevant for isotropic media (liquids or polycrystalline solids). In addition to the intermolecular effects, we will also study how small intramolecular changes within a free water molecule affect the Compton profile. The present work has a connection to recently published x-ray absorption and x-ray Raman scattering studies on the molecular arrange-

ment in the first coordination shell of liquid water.^{11,12} Wer-net *et al.*¹² find evidence that the local coordination around individual molecules may be greatly changed between ice and liquid water. In the present work we aim to show that these kinds of predictions for the local coordination can be studied using the x-ray Compton scattering technique.

As the main findings of the present paper we demonstrate that the isotropic Compton profile is sensitive to the number and distance of molecules/atoms in the first coordination shell around an individual water molecule. The predominant interaction mechanism that affects the profile is found to be the exchange interaction. However, polarization and especially charge transfer are also found to play a role. The results are potentially significant for the analysis of a wide variety of chemically and biologically interesting systems. In order to apply Compton spectroscopy to these systems, it is essential to evaluate the sensitivity of the Compton profile to the above-mentioned subtle changes in the electronic structure.

II. THEORY AND MODEL SYSTEMS

In the present work we employ real-space electronic structure calculations to evaluate the momentum density $N(\mathbf{p})$ and the Compton profile $J(q)$. In order to solve the electronic structure of the model clusters we use density-functional theory¹³ (DFT) utilizing linear combinations of contracted Gaussian basis functions for the Kohn-Sham (KS) equations. The calculations are performed using the computer program StoBe-deMon.¹⁴ In the gradient-corrected exchange-correlation functional the correlation part is that of Perdew *et al.*¹⁵ and the exchange part that of Hammer *et al.*¹⁶ For oxygen we employ a triple-zeta valence plus polarization type basis set, and for hydrogen a primitive set¹⁷ augmented by one p -function in a $[3s, 1p]$ contraction. For neon we use a double-zeta valence plus polarization type basis set.

For the water monomer and dimer we have also performed calculations using the Hartree-Fock approximation and Møller-Plesset second-order perturbation theory.¹⁸ The computations are based on the linear combination of atomic orbitals (LCAO) method with the quantum-chemistry program DALTON.¹⁹ In these calculations we have used the cc-pVTZ basis set.

The momentum density is calculated as a Fourier transform of the real-space density matrix:

$$N(\mathbf{p}) = (2\pi)^{-3} \int d\mathbf{r} d\mathbf{r}' e^{-i\mathbf{p}\cdot(\mathbf{r}-\mathbf{r}')} \rho(\mathbf{r}, \mathbf{r}'), \quad (1)$$

where for the density matrix $\rho(\mathbf{r}, \mathbf{r}')$ we use the system's Kohn-Sham orbitals,

$$\rho(\mathbf{r}, \mathbf{r}') = 2 \sum_i \psi_i(\mathbf{r}) \psi_i^*(\mathbf{r}'), \quad (2)$$

where $\psi_i(\mathbf{r})$ is the i :th KS orbital. The sum above is over the occupied electronic states and the factor 2 accounts for the spin degeneracy. The KS orbitals are expanded using a set of basis functions ϕ_k ,

$$\psi_i(\mathbf{r}) = \sum_k C_{i,k} \phi_k(\mathbf{r} - \mathbf{R}_k), \quad (3)$$

where $C_{i,k}$ are the expansion coefficients and $\phi_k(\mathbf{r} - \mathbf{R}_k)$ denotes the k :th basis function centered on a nucleus at \mathbf{R}_k . Although in DFT the KS orbitals are formally only auxiliary functions, they have been successfully used as approximations for the true wave functions for various wave function derived quantities in Compton,^{5,7} positron annihilation²⁰ and x-ray absorption²¹ spectroscopies. In the case of Compton scattering from the water dimer, Ghanty *et al.*⁶ tested DFT against the Hartree-Fock method for the anisotropies in the directional Compton profile. Both approaches gave very similar results, which demonstrated that DFT includes the exchange interaction to a reasonable accuracy.

Using Eq. (2), the integral of Eq. (1) can be written as

$$N(\mathbf{p}) = 2 \sum_i |\psi_i(\mathbf{p})|^2, \quad (4)$$

where $\psi_i(\mathbf{p})$ is the Fourier transform of the KS orbital,

$$\psi_i(\mathbf{p}) = (2\pi)^{-3/2} \sum_k C_{i,k} \int d\mathbf{r} e^{-i\mathbf{p}\cdot\mathbf{r}} \phi_k(\mathbf{r} - \mathbf{R}_k). \quad (5)$$

In isotropic systems the Compton profile is calculated as spherically averaged over all orientations of the scattering vector relative to the coordinate system fixed at the scatterer. The profile can be written as^{1,2}

$$J(q) = \frac{1}{2} \int_{|q|}^{\infty} \frac{I(p)}{p} dp, \quad (6)$$

where q is a scalar momentum variable and $I(p)$ the spherical average of $N(\mathbf{p})$,

$$I(p) dp = \int_0^{2\pi} \int_0^{\pi} N(\mathbf{p}) \sin \theta d\theta d\phi p^2 dp. \quad (7)$$

In line with the approaches used in the previous studies,⁶⁻⁸ we construct our model systems by applying the local fourfold-coordinated structure of ice *Ih*, where the O-O distance $R_{\text{OO}}^{\text{ice}} = 2.75 \text{ \AA}$. We study the following cases: (i) A free water molecule; (ii) a water dimer, a water-neon dimer and a neon dimer at different interparticle separations R_{OO} , R_{ONe} and R_{NeNe} , respectively; (iii) a water molecule surrounded by a coordination shell of $n=0 \cdots 4$ water molecules at $R_{\text{OO}}^{\text{ice}}$ with the removed $(4-n)$ water molecules put at a distance of $R_{\text{OO}}^{\text{rem}} = 8 \text{ \AA}$ (Model 1A) and $R_{\text{OO}}^{\text{rem}} = 4 \text{ \AA}$ (Model 1B); (iv) a water molecule surrounded by $n=0 \cdots 4$ neon atoms at $R_{\text{ONe}}^{\text{ice}} = 2.75 \text{ \AA}$ with the removed $(4-n)$ neon atoms put at a distance of $R_{\text{ONe}}^{\text{rem}} = 8 \text{ \AA}$ (Model 2A) and $R_{\text{ONe}}^{\text{rem}} = 4 \text{ \AA}$ (Model 2B). Table I summarizes the relevant distances in the model systems.

In the model clusters the value of n thus denotes the coordination number and the case $n=4$ corresponds to the ideal fourfold-coordinated ice-like structure around the central molecule. Note that in ice the two protons of the central molecule are oriented towards two of the neighboring molecules (donor H bonds) and the two protons of two of the neighboring molecules point towards the central one (accep-

TABLE I. Specification of the model clusters for the first coordination shell around a water molecule. n water molecules (neon atoms) are at the R_{OO}^{ice} (R_{ONe}^{ice}) distance from the central water molecule, and $4-n$ water molecules (neon atoms) at the distance of R_{OO}^{rem} (R_{ONe}^{rem}) from the central water molecule.

Model	System	R_{OO}^{ice} or R_{ONe}^{ice} (Å)	R_{OO}^{rem} or R_{ONe}^{rem} (Å)
1A	$\text{H}_2\text{O} \cdot (\text{H}_2\text{O})_n$	2.75	8.0
1B	$\text{H}_2\text{O} \cdot (\text{H}_2\text{O})_n$	2.75	4.0
2A	$\text{H}_2\text{O} \cdot \text{Ne}_n$	2.75	8.0
2B	$\text{H}_2\text{O} \cdot \text{Ne}_n$	2.75	4.0

tor H bonds). For a given hydrogen-bonded pair of two water molecules, we denote the one from which a proton is donated towards the oxygen of the other molecule as the donor molecule. The molecule accepting the hydrogen is called the acceptor molecule. According to a practical classification scheme,²² distances >3.2 Å can be considered to represent “weak” hydrogen bonds, whereas bond lengths around 2.75 Å as in ice correspond to “moderate” ones. Model 1B ($R_{OO}^{\text{rem}}=4$ Å) thus corresponds to a situation where “weak” hydrogen bonds are systematically switched to ‘moderate’ ones. For model 1A ($R_{OO}^{\text{rem}}=8$ Å), as well as for model 2A ($R_{ONe}^{\text{rem}}=8$ Å), the interaction between the central molecule and the distant ligand becomes vanishingly small; too small to be observed in the Compton profile as will be seen in Secs. III A and III B.

III. RESULTS AND DISCUSSION

A. Free water molecule and dimer

In order to get an insight how the different orbitals contribute to the total Compton profile we first study the free water molecule. We use the experimental geometry with the O-H bond length of 0.957 Å and the H-O-H angle of 104.52° (Ref. 23). Figure 1 shows the orbital decomposition of the Compton profile. Except for the $1a_1$ orbital, the orbitals contribute mainly at the peak of the profile at $|q| < 2$ a.u. At higher momenta the broad profile originating from the $1a_1$ core level is clearly separated from the valence contributions.

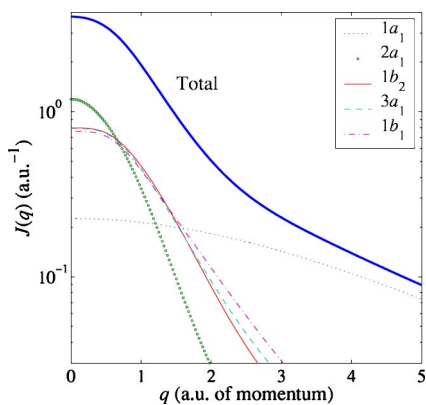


FIG. 1. (Color online) Compton profile for a free water molecule and the contributions from the different orbitals.

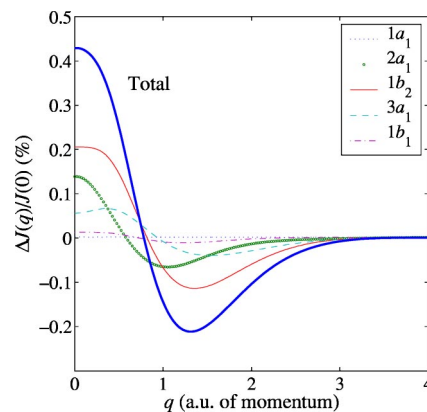


FIG. 2. (Color online) Compton profile difference between a water molecule where the O-H bond length has been increased by 2% and the reference molecule. The contributions from the different orbitals are also shown.

Figure 2 shows a model calculation for the effect of increasing the internal O-H bond length by 2%. Since in general the effects on the profile are relatively small, for clarity the result is shown as a difference curve with respect to the theoretical profile for the free molecule shown in Fig. 1. Figure 2 now readily indicates that the profile becomes slightly narrower and the maximum effect, $\sim 0.5\%$, can be found at the peak of the profile. The narrowing of the profile is due to the relaxation of the $2a_1$, $1b_2$, and $3a_1$ orbitals, which become more spatially expanded following the increase of the proton distances. In momentum space this shows up as a decrease of the average momentum of these orbitals. The $1b_1$ lone-pair orbital with a strong p character does not participate in the O-H bonding and is thus very weakly affected. The $1b_1$ core orbital is, as expected, completely unchanged upon the elongation of the O-H bond. The data thus shows a clear difference even for a very small structural change.

The water dimer can be considered as an elementary model system to study the perturbations induced in the wave functions of the free molecule upon condensation. We consider the ice-like ($R_{OO}=R_{OO}^{\text{ice}}=2.75$ Å) and gas-phase ($R_{OO}=2.98$ Å) dimers as well as the cases $R_{OO}=4.0$ Å and 8.0 Å. The intermolecular geometry corresponds to that used by Ghanty *et al.*,⁶ based on the experimental geometry of the gas-phase dimer,²⁴ and the intramolecular geometry is as in the free molecule case. We have verified that at R_{OO}^{ice} our DFT calculations reproduce the observation by Ghanty *et al.*⁶ for the anisotropy in the directional Compton profiles (difference between the $\text{O} \cdots \text{O}$ direction and that perpendicular to the mirror plane of the dimer). This behavior is a manifestation of the “bond oscillation principle”.⁹

Figure 3(a) gives the difference in the isotropic Compton profiles between the various dimers and two free molecules. Also in this case the resulting difference profile has a clear oscillatory behavior. The positions of the maxima/minima of the difference curve can be seen to depend on the distance R_{OO} between the molecules. The overall effect is a consequence of the bond-induced oscillations of the valence electron wave functions in the momentum space. The deep $1a_1$

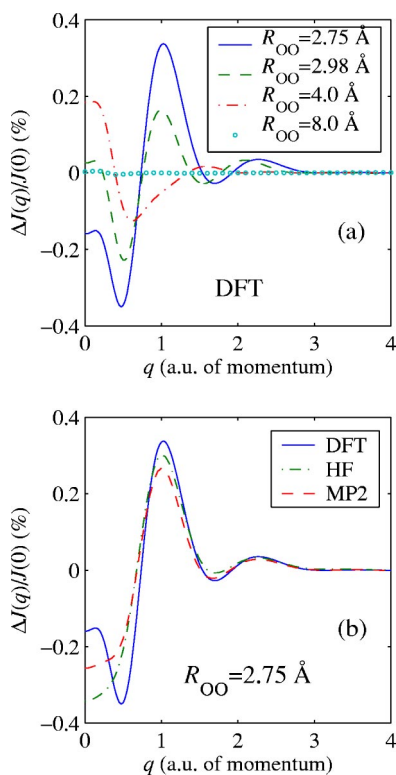


FIG. 3. (Color online) (a) Compton profile differences between water dimers at different separations R_{OO} and two free water molecules. (b) Compton profile differences between a water dimer with $R_{OO}=2.75$ Å and two free water molecules with DFT, LCAO-HF and LCAO-MP2 theories.

core states of the two molecules interact very weakly, constituting the broad, invariant background, which is practically nonexistent in the difference curves. It is thus clear that the “bond oscillation principle”⁹ is manifested also in the isotropic profiles, albeit reduced in magnitude (the amplitude of the oscillations is roughly an order of magnitude smaller). Note that in the DFT results a small oscillation at $|q| < 0.6$ a.u. can also be observed, similar to the one observed in the directional anisotropy.⁶ It is noteworthy that a significant effect in the profile remains at $R_{OO}=4.0$ Å. This will be further seen to affect the results for Models 1B and 2B in Sec. III B. At $R_{OO}=8.0$ Å the effect vanishes, and the profile approaches that of two free water molecules.

For the ice-like dimer $R_{OO}=R_{OO}^{ice}$ the amplitude of the oscillations is of the order of ~ 0.2 – 0.4% at maximum. For the gas phase dimer ($R_{OO}=2.98$ Å) the oscillations are qualitatively similar but smaller in amplitude, and the frequency of the oscillations is slightly higher. Moreover, the DFT results are seen to be rather close to the HF and MP2 results [Fig. 3(b)], except at the lowest momenta, $|q| < 0.5$ a.u., where the profiles are the most sensitive to the used theory [the discrepancy is $\sim 0.2\%$ of $J(0)$]. Our test calculations also indicate that in this region the difference profile is the most sensitive to the choice of the basis set and to small changes in the intra- and intermolecular geometries. We conclude that the isotropic Compton profiles, although averaged over all orientations of the scattering vector, distinctly preserve the bond-related information observed in the directional profiles.

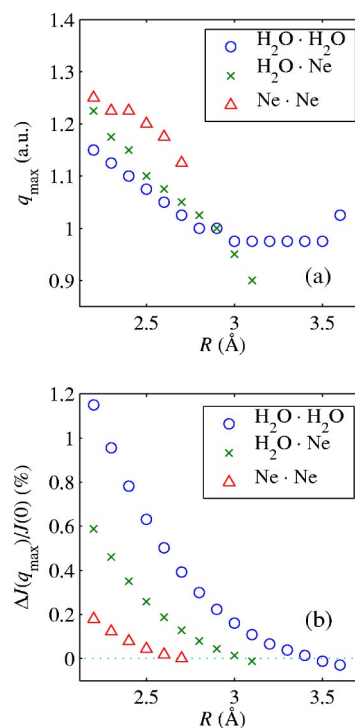


FIG. 4. (Color online) (a) Position q_{max} of the first maximum at ~ 1 a.u. in the difference Compton profiles between dimers at different separations R and the corresponding free molecules/atoms. The results are given for the $(H_2O)_2$, $H_2O \cdot Ne$ and Ne_2 dimers. (b) Value of $\Delta J(q)/J(0)$ at $q=q_{max}$.

We have also studied a $H_2O \cdot Ne$ dimer and a Ne_2 dimer. Replacing a water molecule by a neon atom is expected to give a qualitatively similar “fingerprint” in the momentum density and Compton profile,⁶ but due to a lower polarizability of neon and a smaller atomic radius compared to the molecular radius of the water molecule, the magnitude of the signal is expected to be smaller. When compared to the $(H_2O)_2$ dimer, these systems produce qualitatively similar difference curves when the profiles from the corresponding free molecules/atoms are subtracted, in accordance with the observation by Ghanty *et al.*⁶ These similarities are also further discussed in Sec. III B. In all the cases the largest effects in the difference Compton profile as a function of the intermolecular distance R can be found at $|q| < 0.25$ a.u. (peak of the profile), $|q| \sim 0.5$ a.u. (first minimum) and $|q| \sim 1$ a.u. (first maximum). To extract a quantitative trend, in Fig. 4 we study how the first maximum around $|q| \sim 1$ a.u. behaves as a function of R in the range 2.2–3.6 Å. For the difference Compton profiles for the three dimers the position of the first maximum moves towards lower values of $|q|$ as a function of R until the position cannot anymore be resolved. The value at the first maximum decreases systematically as R increases. It should be noted that in this comparison we used the intermolecular geometries in accordance with the nearest-neighbor arrangement in the ice *Ih* crystal. The H-O-H angle of the water molecules is 109.47° and the O-H bond length is chosen to be 0.950 Å. This geometry will also be used for the model clusters in Sec. III B. The small differences between the two geometries for the dimer have a negligible effect

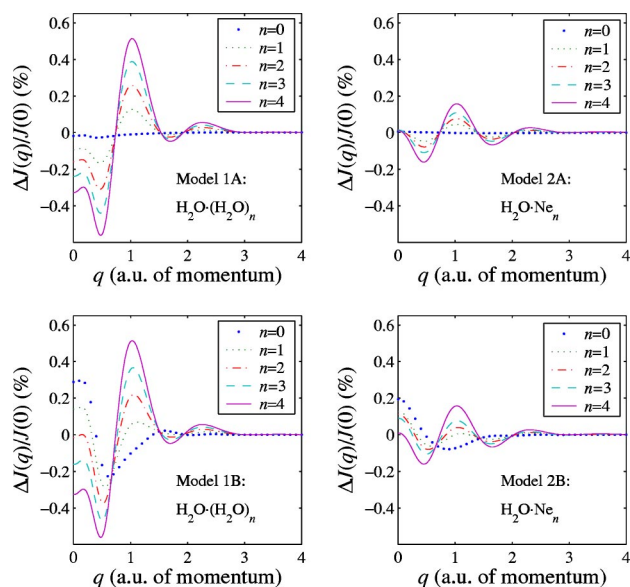


FIG. 5. (Color online) Compton profile differences between the five-molecule model clusters of Table I and the corresponding free molecules/atoms.

when considering the difference profiles between the dimers and the free molecules/atoms, the discrepancy being the largest at $|q| < 0.25$ a.u. [less than 0.05% of $J(0)$].

B. Model clusters

In order to study the effect of coordination on the Compton profile, we turn now to the more complicated local structures by using water and mixed water-neon clusters. Figure 5 shows the effect induced in the Compton profile by various numbers of ligands around the central water molecule in the four model systems specified in Table I. The water molecules have the O-H bond length of 0.950 Å and the H-O-H angle of 109.47°. The plot shows the difference Compton profiles, where the reference profile for models 1A and 1B is that of five free water molecules and for model 2A and 2B that of one free water molecule and four free neon atoms.

For all the four models there are clear effects induced in the Compton profile in the different coordinations. For all models the qualitative trend is rather similar. For the cases $n > 0$ the systems exhibit similar oscillations with six (models 1A, 1B) and five (models 2A, 2B) distinct extrema between the momenta 0 and 2.5 a.u. (the peak at 0 a.u. included). Models 1A and 2A show a systematic effect induced in the profile as the ligands are brought from a distance of 8 Å to the coordination shell. At $n=0$, the interaction between the central molecule and the ligands is vanishingly small. The behavior as a function of n can again be explained by the “bond oscillation principle”.⁹ each of the n ligands are located at the same distance from the central molecule and thus give rise to iso-amplitude and-frequency oscillations in the momentum density along the specific bond directions. If the ligand-ligand (i.e. next-nearest-neighbor) interaction is assumed to be small, as well as the effects due to the non-

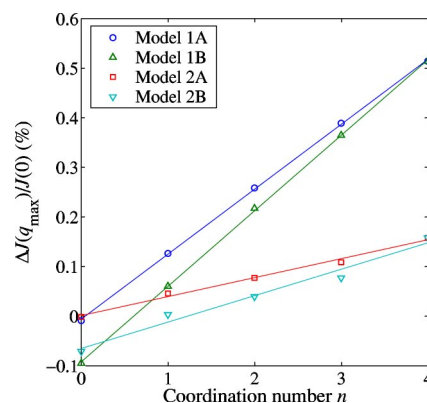


FIG. 6. (Color online) Value of $\Delta J(q)/J(0)$ at q_{\max} for the five-molecule model clusters of Table I. $q_{\max}=1.025$ a.u. is the position of the first maximum in the difference Compton profiles (Fig. 5). The point (0,0) corresponds to the free molecules/atoms. The lines are linear fits to the data.

sphericity of the water molecule, the resulting Compton profile contains n times the signal from a dimer.

Models 1B and 2B ($R_{\text{OO}}^{\text{rem}}, R_{\text{OO}}^{\text{rem}}=4$ Å) show also large effects depending on the coordination number. However, it is clear that now there remains a substantial interaction between the central molecule and the ligand at $R=4$ Å. This effect can be best discerned at $J(0)$. We have also studied the case where a neon atom is surrounded by a shell of other neon atoms similarly as in the models 2A and 2B. This system produced effects less than 0.02% of $J(0)$ even for $n=4$. Thus, for a neon-neon system at distances of $R=2.75$ Å the deformation of the free-atom wave functions is much smaller than in the other cases and beyond the present experimental detection limit.

From the structural point of view, for the coordination number $n=2$ ($n=3$) there are three (two) nonequivalent possibilities to place the ligands around the central water molecule due to the nonequivalence of the donor and acceptor sides of the molecule. For example, Myneni *et al.*,¹¹ using x-ray absorption spectroscopy and theoretical calculations, observed an asymmetry of the hydrogen bonds on the donor side of the molecules in liquid water. We studied the nonequivalent configurations for the cases $n=2$ and $n=3$ and found that the Compton profiles for these model systems differ by less than $\sim 0.04\%$ of $J(0)$. In the model systems studied here the case $n=2$ is chosen to correspond to the situation where one ligand at the donor side and one ligand at the acceptor side are at the distance of $R_{\text{OO}}^{\text{icc}}$ or $R_{\text{ONe}}^{\text{icc}}$ from the central molecule. For $n=3$ one ligand at the donor side and two ligands at the acceptor side are at the distance of $R_{\text{OO}}^{\text{icc}}$ or $R_{\text{ONe}}^{\text{icc}}$.

To better resolve the trends in the profiles for the different models, in Fig. 6 we plot the values $\Delta J(q)/J(0)$ at the position of the first maximum, $q_{\max}=1.025$ a.u., as a function of the coordination number. The point (0,0) corresponds to the free molecules/atoms. Models 1A and 1B show an essentially linear behavior as a function of n . For models 2A and 2B with neon atoms as ligands the trend is also linear but the slope is less steep. As discussed above, the models 1B and 2B contain a significant interaction over the distance of R

TABLE II. Constrained space orbital variation calculation for the water dimer at $R_{OO}^{\text{ice}}=2.75$ Å. ΔE gives the change of energy compared to two free water molecules. ΔE_{step} denotes the change of energy compared to the previous CSOV step.

CSOV step	ΔE (eV)	ΔE_{step} (eV)
0. Free H ₂ O molecules	0	-
1. Frozen config.	+0.076	+0.076
2. Polarization	+0.014	-0.062
3. Full relaxation	-0.149	-0.163

=4 a.u., leading to values $\Delta J(q)/J(0)$ below zero at q_{max} for $n=0$.

We have thus seen that the main feature upon adding 1–4 ligands at the distance $R=2.75$ Å from the central water molecule is the generation of iso-amplitude and -frequency oscillations in the isotropic Compton profile. In accordance with the previous studies,^{6–8} the most straightforward method is to associate the oscillations to the exchange interaction. The water-water and the water-neon systems are found to produce oscillations with a different amplitude, but with similar positions of the maxima/minima. The smaller amplitude of the oscillations in the water-neon system can be explained by the lower polarizability of neon and the smaller extent of the radius of the neon atom as compared with the radius of the water molecule, leading to a smaller exchange interaction. Moreover, the charge transfer component (HOMO-LUMO mixing) is absent for the water-neon system.

In order to study more quantitatively the effects of exchange, polarization and charge transfer on the Compton profile, we have carried out a constrained space orbital variation (CSOV) analysis²⁵ of the water dimer. The change of energy and the Compton profile at each CSOV step is compared to the case of two free water molecules (Table II and Fig. 7). In the first CSOV step (frozen configurations), two free water molecules are brought to the distance of $R_{OO}=R_{OO}^{\text{ice}}$ and only the electrostatic and exchange interactions between the molecules are allowed. The change of energy is slightly positive, which indicates that the exchange repulsion

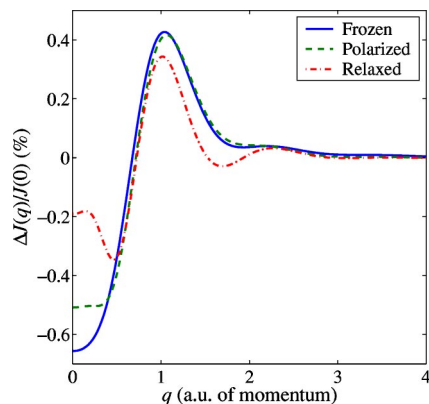


FIG. 7. (Color online) Compton profile differences at the various stages of the CSOV analysis between a water dimer with $R_{OO}=2.75$ Å and two free water molecules.

is larger than the electrostatic attraction between the dipoles. In contrast, a large oscillatory feature is induced in the Compton profile.

In the second CSOV step the internal polarization of both molecules is added. Initially, one molecule is allowed to polarize while the second molecule is kept frozen. Then the polarization of the second molecule is added while the first molecule is kept frozen. The procedure is repeated until the total energy and the Compton profile have converged. After this step the energy is slightly decreased and the peak height of the Compton profile is increased. The final CSOV step allows the charge transfer (i.e., full orbital mixing) between the two molecules. Only after this step does the system become energetically stable. Most of the energy gain comes from the charge transfer from the acceptor molecule to the donor one. At this step the Compton profile is also notably changed: the peak height of the profile is strongly increased and the oscillatory feature is modified. Nevertheless, the oscillatory feature governs the character of the profile.

We may understand the changes in the Compton profile upon H-bond formation as follows. The exchange interaction leads to an initial repulsion and creates the large oscillatory feature in the Compton profile due to the overlap of the occupied orbitals. Internal polarization does not lead to a significant lowering of energy, which is concurrent with the weak effect on the Compton profile at the second CSOV step. For the dimer to overcome the exchange repulsion and to be energetically stable, charge transfer and subsequent orbital rearrangements take place.²⁶ This is reflected in a qualitative change of the Compton profile between the second and the third CSOV step.

The studied model systems for the water and mixed water-neon clusters as well as for the dimers show that the Compton profile is indeed highly sensitive to the local environment of an individual water molecule. The existence of an observable signal in the profile when the distance of the ligands from the central water molecule is 4 Å is important, suggesting that the coordination shell properties of water molecules can be probed over relatively large distances.

Our preliminary experiments confirm that the predicted subtle intra- and intermolecular effects, typically of the order of a fraction of percents at $J(0)$, can be detected in the Compton profile as concerns the statistical and systematic errors in the experimental data measured using a synchrotron-radiation source.²⁷ The induced oscillatory changes in the Compton profiles are rather slowly varying so that even a moderate experimental momentum resolution of about 0.5 a.u. is adequate to detect the predicted effects. To this end, one can use a multi-element solid-state detector (0.1 a.u. bin size) with a high efficiency. This setup is found to provide a statistical accuracy of better than 0.02% at the Compton peak from ice and liquid water samples.²⁷

We have also verified that our predictions for the changes in the Compton profile are in a qualitative agreement with those reported by Barbiellini and Shukla,¹⁰ who used the Hartree-Fock method. Following their work, we have studied the negative radial derivative $-dN(p)/dp$ of the isotropic momentum density $N(p)$ for the free molecule, the dimer and the H₂O·(H₂O)₄ cluster. We observe a qualitatively similar trend as they for the position of $-dN(p)/dp$ and for the quan-

tity Δp [full width at half maximum of $-dN(p)/dp$]. The amount of charge transferred, evaluated using Eqs. (1), (6), and (7) of Ref. 10, is about 0.3% of an electron in the dimer and 1.1% in the $\text{H}_2\text{O}\cdot(\text{H}_2\text{O})_4$ cluster. The value in the dimer agrees fairly well with the corresponding value of 0.5% reported in Ref. 10. The slight discrepancy presumably reflects the different theoretical approaches. This comparison is another indication that there are systematic changes in the Compton profile when the coordination number of individual molecules increases.

In the present work we have considered only highly symmetric geometries. In the case of liquid water, distortions in the hydrogen bond geometry around each molecule are expected (stretching, bending and breaking of bonds). As Figs. 3(a) and 4(b) (dimers) and Fig. 5 (clusters) show, linear stretching of the hydrogen bond decreases the amplitude of the oscillations in the difference Compton profile. In contrast, the positions of the first minimum and the first maximum do not change drastically upon stretching. Consequently, there can be only minor cancellation effects in the Compton profile if the system contains hydrogen bonds with varied bond lengths. Our preliminary calculations for dimers and small clusters suggest that this is also the case for bent (i.e., nonlinear) hydrogen bonds. Therefore, independent of the variations in the hydrogen bond geometry, each bond donated or accepted by an individual water molecule is expected to contribute constructively to the total oscillatory feature. For liquid water we hence expect a comparable oscillatory signal in the Compton profile as a function of the coordination number and distance of the molecules in the first coordination shell. Compton scattering may thus provide important insight into the structure of liquid water in different conditions (temperature and pressure effects, solvation-induced structures).

IV. CONCLUSIONS

We have conducted a density-functional study of the isotropic Compton profiles for a set of closed-shell model systems. Water and mixed water-neon clusters have been used as test cases, with intermolecular distances typical of ice. LCAO-HF and -MP2 calculations have also been performed for the free water molecule and the water dimer. The calculations for the free water molecule show that an elongation of the intramolecular covalent O-H bond can be distin-

guished as a narrowing of the profile. The narrowing is due to the decrease of the average momentum of the orbitals forming the bond. A 2% elongation was found to lead to a predicted 0.5% increase at the peak of the profile.

For the water, water-neon and neon dimers, the isotropic Compton profile exhibits oscillations as compared with the profile from the corresponding free molecules/atoms. The oscillations are similar to those observed in the anisotropy of the directional Compton profiles for the water and water-neon dimers, which shows that the isotropic profiles contain similar information. In terms of different classes of hydrogen bonds,²² the present results suggest that “strong” ($R_{\text{OO}} < 2.5 \text{ \AA}$) and “moderate” ($2.5 \text{ \AA} < R_{\text{OO}} < 3.2 \text{ \AA}$) hydrogen bonds can be detected in the profile, but to some extent also “weak” ones ($R_{\text{OO}} > 3.2 \text{ \AA}$). The detection of the hydrogen bond in water requires, however, a high statistical accuracy that can be achieved by the use of synchrotron radiation.

The results for the five-molecule clusters for the first coordination shell show that the isotropic Compton profiles are sensitive both to the number and distance of the water or neon ligands around the central water molecule. Each ligand which is brought to the coordination shell at $R=2.75 \text{ \AA}$ is found to add to the systematic oscillatory feature in the profile. For water clusters this feature is in essence the signature of the hydrogen bond. Replacing the water molecules by neon atoms in the coordination shell reduces the effect in the profile. This is interpreted as a weaker exchange interaction due to the smaller spatial extent of the wave function of neon compared to the wave function of the water molecule.

The CSOV analysis for the water dimer shows that in addition to the exchange interaction, charge transfer modifies the Compton profile, while the role of polarization is weak. The findings suggest that isotropic Compton profiles may provide an important insight into the study of the local coordination of closed-shell atoms and molecules. To test and apply these findings, we propose further Compton scattering experiments on ice and liquid water under different conditions as well as experiments on free water clusters and ionic solvation.

ACKNOWLEDGMENTS

This work has been supported by the Academy of Finland (Contracts No. 201291/40732). LGMP and AN thank the Swedish Foundation for Strategic Research (SSF) and the Swedish Research Council (VR) for financial support.

*Electronic address: Mikko.O.Hakala@helsinki.fi

†Corresponding author.

‡Present address: European Synchrotron Radiation Facility, Boîte Postale 220, F-38042 Grenoble Cedex 9, France.

§Present address: BESSY, Albert-Einstein-Strasse 15, D-12489 Berlin, Germany.

¹B. G. Williams, in *Compton Scattering* (McGraw-Hill, London, 1977).

²M. J. Cooper, *Rep. Prog. Phys.* **48**, 415 (1985).

³P. Eisenberger and P. M. Platzman, *Phys. Rev. A* **2**, 415 (1970).

⁴See, for example, M. Nyberg, M. Odellius, A. Nilsson, and L. G. M. Pettersson, *J. Chem. Phys.* **119**, 12577 (2003).

⁵E. D. Isaacs, A. Shukla, P. M. Platzman, D. R. Hamann, B. Barbiellini, and C. A. Tulk, *Phys. Rev. Lett.* **82**, 600 (1999).

⁶T. K. Ghanty, V. N. Staroverov, P. R. Koren, and E. R. Davidson, *J. Am. Chem. Soc.* **122**, 1210 (2000).

⁷A. H. Romero, P. L. Silvestrelli, and M. Parrinello, *J. Chem. Phys.* **115**, 115 (2001).

- ⁸S. Ragot, J.-M. Gillet, and P. J. Becker, *Phys. Rev. B* **65**, 235115 (2002).
- ⁹I. R. Epstein and A. C. Tanner, in Ref. 1, p. 209.
- ¹⁰B. Barbiellini and A. Shukla, *Phys. Rev. B* **66**, 235101 (2002).
- ¹¹S. Myneni, Y. Luo, L. Å. Näslund, M. Cavalleri, L. Ojamäe, H. Ogasawara, A. Pelmenchikov, Ph. Wernet, P. Väterlein, C. Heske, Z. Hussain, L. G. M. Pettersson, and A. Nilsson, *J. Phys.: Condens. Matter* **14**, L213 (2002).
- ¹²Ph. Wernet, D. Nordlund, U. Bergmann, M. Cavalleri, M. Odelius, H. Ogasawara, L. Å. Näslund, T. K. Hirsch, L. Ojamäe, P. Glatzel, L. G. M. Pettersson, and A. Nilsson, *Science* **304**, 995 (2004).
- ¹³P. Hohenberg and W. Kohn, *Phys. Rev.* **136**, B864 (1964); W. Kohn and L. J. Sham, *ibid.* **140**, A1133 (1965).
- ¹⁴StoBe-deMon version 1.0, K. Hermann and L. G. M. Pettersson, M. E. Casida, C. Daul, A. Goursot, A. Koester, E. Proynov, A. St-Amant, and D. R. Salahub. Contributing authors: V. Caravetta, H. Duarte, N. Godbout, J. Guan, C. Jamorski, M. Leboeuf, V. Malkin, O. Malkina, M. Nyberg, L. Pedocchi, F. Sim, L. Triguero, and A. Vela, StoBe Software, 2002. <http://w3.rz-berlin.mpg.de/~hermann/StoBe/index.html>
- ¹⁵J. P. Perdew, K. Burke, and M. Ernzerhof, *Phys. Rev. Lett.* **77**, 3865 (1999).
- ¹⁶B. Hammer, L. B. Hansen, and J. K. Norskov, *Phys. Rev. B* **59**, 7413 (1999).
- ¹⁷S. Huzinaga, *J. Chem. Phys.* **42**, 1293 (1965).
- ¹⁸C. Møller and M. S. Plesset, *Phys. Rev.* **46**, 618 (1934); J. S. Binkley and J. A. Pople, *Int. J. Quantum Chem.* **9**, 229 (1975).
- ¹⁹T. Helgaker *et al.*, DALTON, a molecular electronic structure program, release 1.2, 2001, <http://www.kjemi.uio.no/software/dalton>.
- ²⁰M. Alatalo, B. Barbiellini, M. Hakala, H. Kauppinen, T. Korhonen, M. J. Puska, K. Saarinen, P. Hautojärvi, and R. M. Nieminen, *Phys. Rev. B* **54**, 2397 (1996).
- ²¹L. Triguero, L. G. M. Pettersson, and H. Ågren, *Phys. Rev. B* **58**, 8097 (1998).
- ²²T. Steiner, *Angew. Chem., Int. Ed.* **41**, 48 (2002).
- ²³W. S. Benedict, N. Gailar, and E. K. Plyler, *J. Chem. Phys.* **24**, 1139 (1956).
- ²⁴T. R. Dyke, K. M. Mack, and J. S. Muenter, *J. Chem. Phys.* **66**, 498 (1977).
- ²⁵P. S. Bagus, K. Hermann, and C. W. Bauschlicher, *J. Chem. Phys.* **80**, 4378 (1984); **81**, 1966 (1984).
- ²⁶A. Nilsson, H. Ogasawara, M. Cavalleri, D. Nordlund, M. Nyberg, Ph. Wernet, and L. G. M. Pettersson (unpublished).
- ²⁷K. Hämäläinen, K. Nygård, S. Huotari, S. Manninen, M. Hakala, and L. G. M. Pettersson (unpublished).